Electron collisions with small esters: A joint experimental-theoretical investigation

G. L. C. de Souza,[1] L. A. da Silva,[2] W. J. C. de Sousa,[3] R. T. Sugohara,[4] I. Iga,[2] A. S. dos Santos,[5] L. E. Machado,[5] M. G. P. Homem,[2] L. M. Brescansin,[6] R. R. Lucchese,[7] and M.-T. Lee[2]

[1]*Departamento de Química, Universidade Federal de Mato Grosso, 78060-900 Cuiabá, Mato Grosso, Brazil*
[2]*Departamento de Química, Universidade Federal de São Carlos, 13565-905 São Carlos, São Paulo, Brazil*
[3]*Instituto de Ciências Exatas e Tecnologia, Universidade Federal do Amazonas, 69100-000 Itacoatiara, Amazonas, Brazil*
[4]*Instituto Federal de Educação, Ciência e Tecnologia de São Paulo, Campus Itapetininga, 18202-000 Itapetininga, São Paulo, Brazil*
[5]*Departamento de Física, Universidade Federal de São Carlos, 13565-905 São Carlos, São Paulo, Brazil*
[6]*Instituto de Física "Gleb Wataghin", Universidade Estadual de Campinas, 13083-970 Campinas, São Paulo, Brazil*
[7]*Department of Chemistry, Texas A&M University, College Station, Texas 77842-3012, USA*

(Received 18 December 2015; revised manuscript received 16 February 2016; published 29 March 2016)

A theoretical and experimental investigation on elastic electron scattering by two small esters, namely, methyl formate and ethyl acetate, is reported. Experimental differential, integral, and momentum-transfer cross sections are given in the 30–1000 eV and 10°–120° ranges. The relative-flow technique was used to determine such quantities. Particularly for methyl formate, a theoretical study was also carried out in the 1–500 eV range. A complex optical potential derived from a Hartree-Fock molecular wave function was used to represent the collision dynamics, whereas the Padé approximation was used to solve the scattering equations. In addition, calculations based on the framework of the independent-atom model (IAM) were also performed for both targets. In general, there is good agreement between our experimental data and the present theoretical results calculated using the Padé approximation. The theoretical results using the IAM also agree well with the experimental data at 200 eV and above. Moreover, for methyl formate, our calculations reveal a $^2A''$ (π^*) resonance at about 3.0 eV and a σ^*-type resonance centered at about 8.0 eV in the $^2A'$ scattering channel. The π^* resonance is also seen in other targets containing a carbonyl group.

DOI: 10.1103/PhysRevA.93.032711

I. INTRODUCTION

The search for renewable energy sources is certainly strategic for all countries in order to control global warming effects. In this regard, the use of biodiesel replacing fossil fuels is an important step. Chemically, biodiesel is a mixture of esters with long carbon chains that can be obtained from vegetable oils or animal fats via transesterification reactions [1]. Therefore, the investigation on electron interactions with small esters such as methyl formate and ethyl acetate may help the understanding of biodiesel combustion process. In addition, small esters have also been observed in interstellar clouds. For instance, methyl formate, together with its isomers, acetic acid, and glycolaldehyde, were detected in hot molecular cores [2]. It is also known that this ester is much more abundant than its isomers with the ratios of 1864:103 and 1864:1 relative to the acetic acid and glycolaldehyde, respectively [3]. Thus, cross sections for electron scattering by these species are important for the understanding of physical and chemical processes in those media [2].

Despite that, there are limited investigations on electron interactions with small esters in the literature. The electron diffraction method was applied to determine the molecular structure of methyl formate [4]. Also, oscillator strengths for C1*s* and O1*s* in methyl formate were measured by Ishii and Hitchcock [5] using an electron energy-loss spectroscopy technique. In addition, total ionization cross sections (TICS) for electron collisions with methyl formate and ethyl acetate were measured by Hudson *et al.* [6] at energies from near threshold to 285 eV.

In the present study we report a joint experimental-theoretical study of electron collisions with two small esters. More specifically, experimental differential (DCS), integral (ICS), and momentum-transfer (MTCS) cross sections for elastic electron scattering by methyl formate and ethyl acetate in the 30–1000 eV energy range are reported. The DCS were determined using the relative-flow technique (RFT), whereas experimental ICS and MTCS were generated from the measured DCS via a numerical integration procedure. Theoretically, the DCS, ICS, MTCS, and the grand-total (TCS) and total absorption (TACS) cross sections for e^--methyl formate collisions were calculated using a combination of the molecular complex optical potential (MCOP) and the Padé approximation. These quantities are reported in the 1–500 eV energy range.

The organization of this work is as follows. In Sec. II we present briefly the experimental procedure. In Sec. III the MCOP theory used and details of the calculations are presented. In Sec. IV we compare our calculated and measured data for methyl formate, whereas our experimental data for ethyl acetate are compared with the results calculated using the independent-atom model (IAM). Finally, in Sec. V we present a summary.

II. EXPERIMENT

Methyl formate and ethyl acetate with purities better than 95% and 99% were purchased from EMD Millipore and Synth, respectively. Details of our experimental setup and procedures were already presented in our previous works [7–14] and therefore will only be outlined here. Angular distributions of elastically scattered electrons were measured in the 30–1000 eV range using a crossed electron-beam–molecular-

beam geometry. In our experiments, electronically inelastic scattered electrons were filtered by using a retarding-field energy analyzer with resolution around 1.5 eV. This resolution does not allow the separation of the vibrationally elastic and inelastic processes, thus the measured intensities are vibrationally summed. Furthermore, the elastically scattered intensities were converted to absolute DCS using the RFT [15]. For that, Ar and N_2 were used as secondary standards. The details for the precise determination of the relative flows for the targets of interest and the secondary standards were given in our previous work [10]. Moreover, the absolute DCS of Ar and N_2 available in the literature [16–18] in the 30–1000 eV range were used to normalize our data. The application of the RFT requires that the beam profiles of the target of interest and secondary standards are almost the same. This condition can be satisfied when the intensities of scattered electrons for these gases at a given angle are measured using the ratio of pressures that ensures the equal mean free path. Nevertheless, as shown in one of our previous works [9], if the scattering intensities are obtained in a pressure region where they are proportional to the gaseous beam flux, the conversion of scattering intensity to the DCS can be made regardless of such ratio of pressures, which is done in this work.

The estimation of uncertainties of the present data was carried out combining the experimental errors of both systematic and random natures [9,14] with the quoted uncertainties for the secondary standards [16–18]. The overall estimated uncertainties are 16.5% at 30 eV, 21% at 50 eV, 15% at 800 and 1000 eV, and 11% at other energies.

The ICS and MTCS were obtained via a numerical integration over the DCS. An extrapolation procedure was used to estimate the DCS at scattering angles not covered experimentally. The trend of the theoretical results was followed in this procedure in order to reduce the arbitrariness. The overall uncertainties on ICS and MTCS were estimated to be 30% at 30 and 50 eV and 25% at other energies.

III. THEORY AND NUMERICAL PROCEDURE

The theory used in this work was already presented in several of our previous articles [14,19–21]. Basically, a molecular complex optical potential composed of static U_{st}, exchange U_{ex}, correlation-polarization U_{cp}, and absorption U_{ab} contributions was used to represent the electron-target interaction. Further, the scattering equations with the MCOP were solved using the Padé approximation [22], which provides the body-frame transition T matrices. Such T matrices were transformed to laboratory-frame scattering amplitudes via an usual frame transformation [23].

TABLE I. Experimental DCS (in 10^{-16} cm^2/sr), ICS (in 10^{-16} cm^2), and MTCS (in 10^{-16} cm^2) for elastic e^--methyl formate scattering. Extrapolated values are given in parentheses.

Angle (deg)	E (eV) 30	50	100	150	200	300	400	500	800
					DCS				
3	(53)	(65)	(75)	(95)	(80)	(78)	(75)	(70)	(60)
5	(51)	(60)	(68)	(71)	(65)	(57)	(56)	(49)	(30)
10	(40)	40.83	26.56	13.84	11.14	11.72	7.39	7.89	3.20
15	23.93	19.56	10.49	4.92	3.76	2.93	2.49	2.62	1.45
20	14.77	8.90	3.04	2.50	1.99	1.42	1.24	1.27	0.875
25	6.73	(3.97)	1.68	1.55	1.19	0.775	0.710	0.907	0.549
30	3.91	1.97	1.03	0.997	0.723	0.549	0.574	0.635	0.283
35	(2.57)	(1.39)	0.739	0.559	(0.54)	0.434	0.398	0.349	(0.19)
40	1.71	0.957	0.519	0.370	0.427	0.319	0.230	0.207	0.121
50	0.958	0.657	0.299	0.261	0.275	0.160	0.123	0.119	0.058
60	0.757	0.437	0.226	0.166	0.158	0.098	0.086	0.081	0.034
70	0.532	0.272	0.156	0.095	0.115	0.083	0.061	0.052	0.024
80	0.431	0.209	0.137	0.083	0.101	0.065	0.043	0.040	0.016
90	0.347	0.189	0.109	0.096	0.093	0.055	0.037	0.034	0.011
100	0.366	0.199	0.109	0.099	0.096	0.055	0.033	0.029	0.009
110	0.440	0.268	0.125	0.101	0.091	0.053	0.031	0.026	0.008
120	0.680	0.358	0.170	0.119	0.087	0.049	0.030	0.024	0.007
130	(0.91)	(0.55)	0.212	0.120	(0.09)	(0.05)	(0.03)	(0.02)	0.006
140	(1.16)	(0.68)	(0.23)	(0.12)	(0.10)	(0.05)	(0.03)	(0.02)	(0.006)
150	(1.44)	(0.83)	(0.27)	(0.12)	(0.11)	(0.05)	(0.03)	(0.02)	(0.006)
160	(1.76)	(0.97)	(0.31)	(0.13)	(0.12)	(0.05)	(0.03)	(0.02)	(0.006)
170	(1.98)	(1.10)	(0.36)	(0.13)	(0.12)	(0.05)	(0.03)	(0.02)	(0.006)
180	(2.19)	(1.16)	(0.38)	(0.14)	(0.12)	(0.05)	(0.03)	(0.02)	(0.006)
					ICS				
	24.6	18.1	11.1	8.5	7.4	6.2	5.3	5.0	3.0
					MTCS				
	11.0	6.3	2.6	1.6	1.5	0.87	0.60	0.52	0.21

In the present work U_{st} and U_{ex} were derived exactly from the target wave function, whereas U_{cp} was obtained in the framework of the free-electron-gas model, derived from a parameter-free local density, as prescribed by Padial and Norcross [24]. Our calculated polarizabilities were used to generate the asymptotic form of U_{cp}.

The absorption potential U_{ab} was generated using the scaled quasifree scattering model of Lee and co-workers [25,26], which is an improvement of the third version of the model absorption potential originally proposed by Staszewska *et al.* [27]. The Hara free-electron-gas-exchange potential [28] was used to generate the local exchange potential U_{ex}^{loc}.

The ground-state Hartree-Fock (HF) self-consistent-field (SCF) wave function of methyl formate was obtained using the triple-zeta valence basis set of GAMESS package [29]. At the experimental molecular geometry [30], this basis provided a total energy of −227.862 862 hartrees, to be compared with the value of −229.157 276 hartrees obtained by using the density-functional theory (DFT) [30]. Our calculated electric dipole moment was 2.084 D, in fairly good agreement with the experimental value of 1.77 D [30]. The dipole polarizabilities calculated at the HF SCF level using the same basis set were $\alpha_{xx} = 28.85$ a.u., $\alpha_{yy} = 27.15$ a.u., and $\alpha_{zz} = 18.64$ a.u., resulting in an average dipole polarizability of $\alpha_0 = 24.88$ a.u., in good agreement with the theoretical value of 26.93 a.u. from the same DFT calculation [30].

In this study the wave functions and interaction potentials, as well as the related matrices, were single-center expanded about the center of mass of the molecule in terms of the symmetry-adapted functions $X_{lh}^{p\mu}$ [31]. The cutoff parameters used in these expansions were $l_c = 30$ and $h_c = 30$ for all bound and continuum orbitals, whereas the T-matrix elements were truncated at $l_c = 28$ and $h_c = 28$ for energies up to 50 eV and at $l_c = 30$ and $h_c = 30$ for higher energies. The calculated cross sections were converged up to ten iterations.

Also, a Born-closure formula was used to account for the contribution of higher partial-wave components of the scattering amplitudes. This procedure, used in some of our previous studies [12,32,33], is necessary due to the slow convergence of T-matrix partial-wave expansion for polar targets.

IV. RESULTS AND DISCUSSION

A. Methyl formate

Our experimental DCS, ICS, and MTCS for elastic electron scattering by methyl formate in the 30–800 eV range are listed in Table I. The extrapolated DCS at angular regions not covered in the experiment were also included. In general, they were obtained following the trend of the MCOP calculations. Nonetheless, for energies higher than 150 eV and angles larger than 120°, the extrapolated DCS were obtained following the trend of the IAM. Comparisons of present experimental DCS with calculated results using the MCOP are shown in Figs. 1–3, along with our results calculated using the IAM as described in Ref. [9]. In general, the MCOP DCS agree well with the present measured results. Nevertheless, at 300 eV and above, the MCOP results underestimate the DCS at large scattering angles. This discrepancy was also observed in our recent electron-acetone scattering study [14]. It is mainly due to the lack of convergence in the single-center expansion of the nuclear part of U_{st} for atoms a few angstroms away from the expansion center. The effects of this lack of convergence are particularly enhanced at high incident energies due to the fact that the scattering electron may penetrate more deeply into the target.

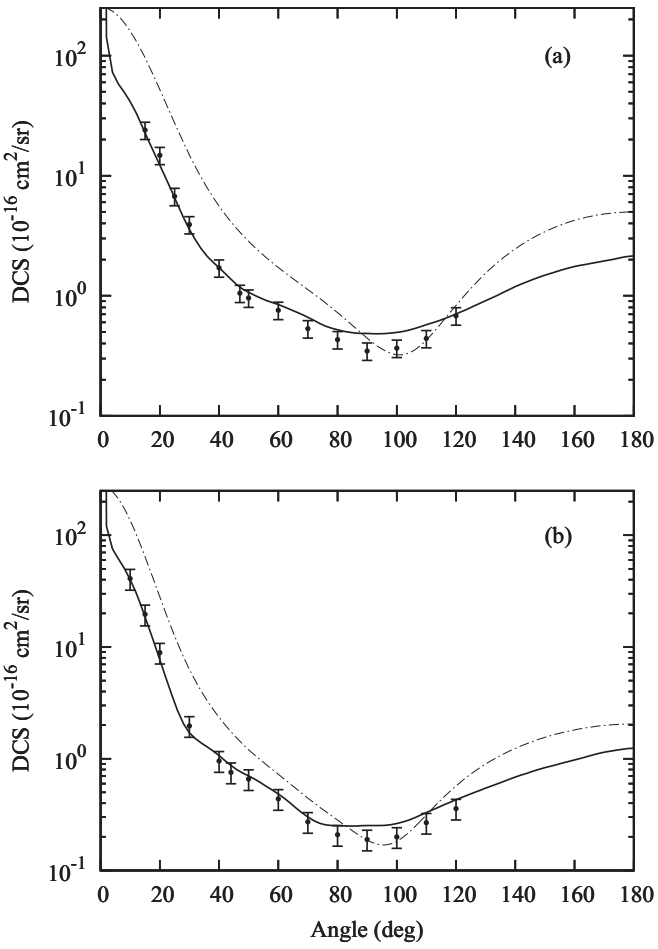

FIG. 1. The DCS for elastic e^--methyl formate scattering at (a) 30 eV and (b) 50 eV: solid curve, present MCOP results; dash-dotted curve, present IAM results; closed circles, present experimental results.

At 150 eV and below, the IAM calculations clearly overestimate the experimental DCS. Nevertheless, such discrepancies decrease with increasing incident energies. It is interesting to note that the theoretical results calculated using the IAM at large scattering angles are in better agreement with the measured data than those of MCOP for energies higher than 300 eV. This is due to the multicentric nature of the interaction potential used in IAM calculations [34].

In Fig. 4 we present our theoretical ICS and MTCS calculated using the MCOP in the 1–500 eV range. The present experimental results of ICS and MTCS in the 30–500 eV range are also shown for comparison. There is very good agreement between our calculated and measured data. Unfortunately, at energies below 30 eV, no other results of ICS and MTCS for this target are available in the literature. On the other hand, a theoretical investigation on electron scattering by acetic acid at energies up to 10 eV was published by Freitas *et al.* [35]. A comparison of their ICS calculated

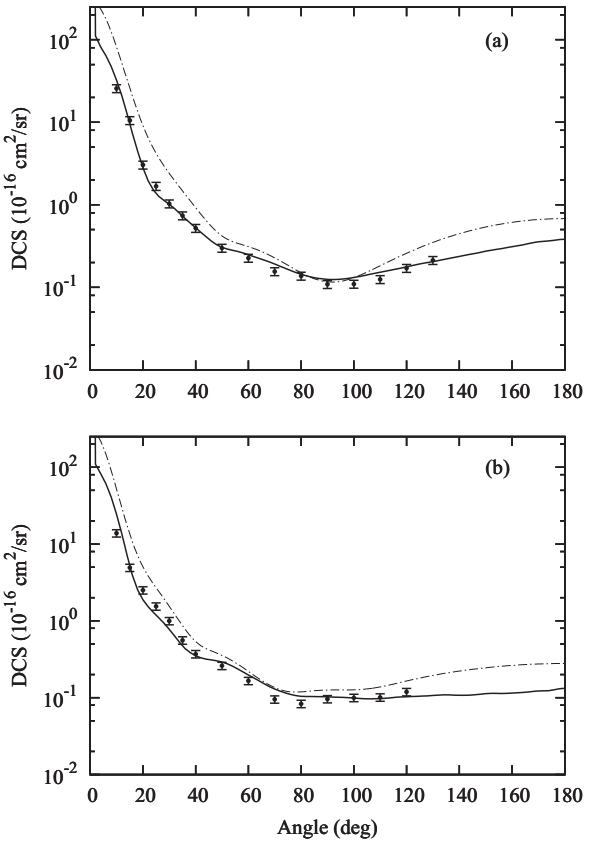

FIG. 2. Same as in Fig. 1 but at (a) 100 eV and (b) 150 eV.

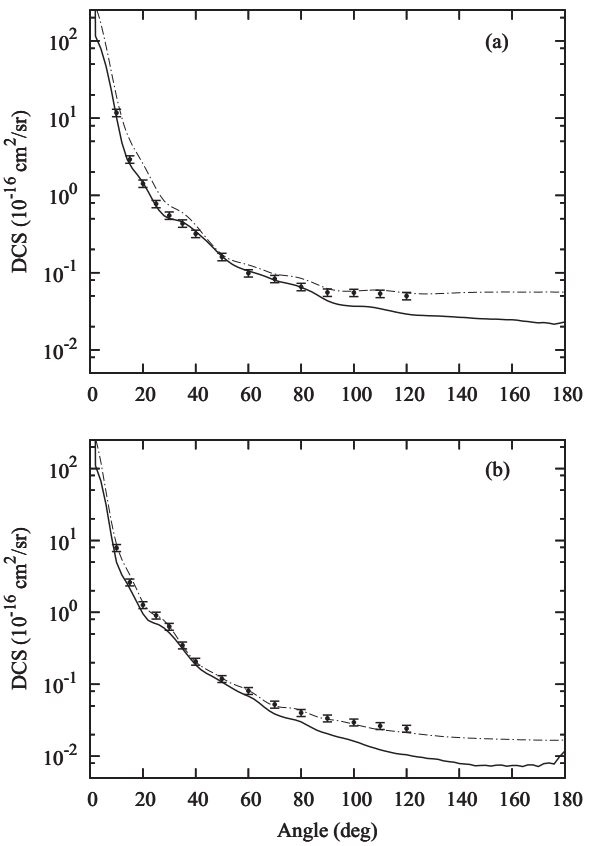

FIG. 3. Same as in Fig. 1 but at (a) 300 eV and (b) 500 eV.

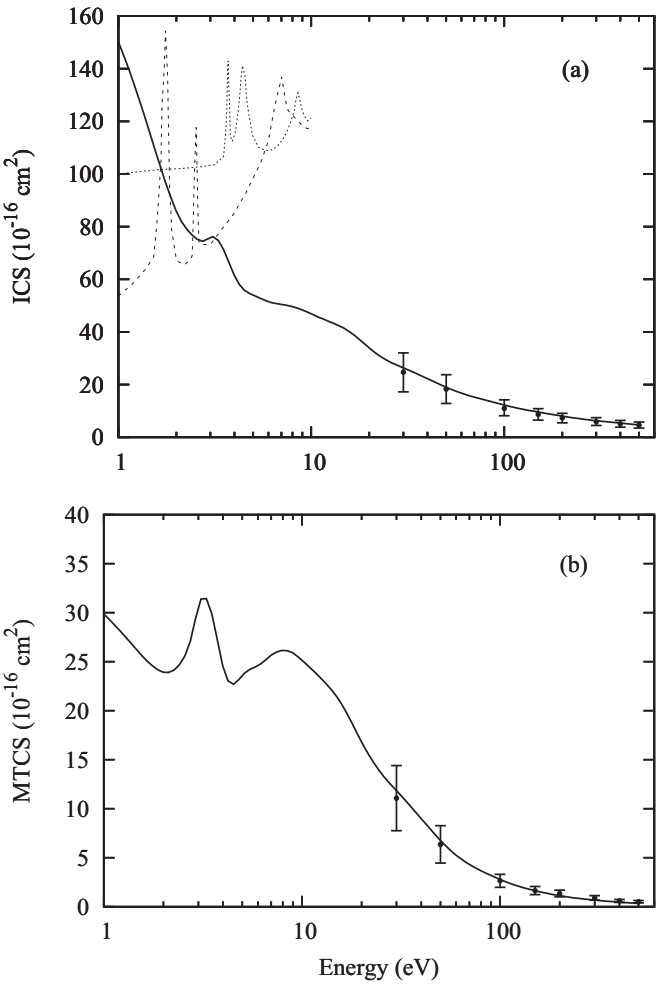

FIG. 4. The (a) ICS and (b) MTCS for elastic e^--methyl formate scattering: solid curve, present calculated data using the MCOP; dashed curve, SMC SEP ICS for the e^--acetic acid scattering of Freitas *et al.* [35]; short-dashed curve, SMC SE ICS for the e^--acetic acid scattering of Freitas *et al.* [35]; closed circles, present experimental data.

using the Schwinger multichannel (SMC) method at static-exchange (SE) and static-exchange-polarization (SEP) levels of approximations [35] with our data may provide some interesting information, since methyl formate and acetic acid are isomers. In this low-energy region, both our MCOP ICS and MTCS show two structures: one peak located at incident energies around 3.0 eV and a broad resonancelike feature centered at about 8 eV. The partial-channel cross-section analysis showed that the first peak is due to a strong $^2A''$ resonance located at 3.0 ± 0.1 eV with a width of 0.8 eV. This resonance is well known in electron scattering studies of targets containing a carbonyl group. In such systems, the empty π^* orbital of that group may trap a low-energy scattering electron to form a metastable ion and thus supports a shape resonance [14,21,36]. This resonance was also identified in the $^2A''$ scattering channel in electron–acetic acid study of Freitas *et al.* [35], located at about 4.2 eV in their SE and 1.8 eV in the SEP calculations. Moreover, the resonance located at about 8.0 eV seen in the present study was identified to have a $^2A'$

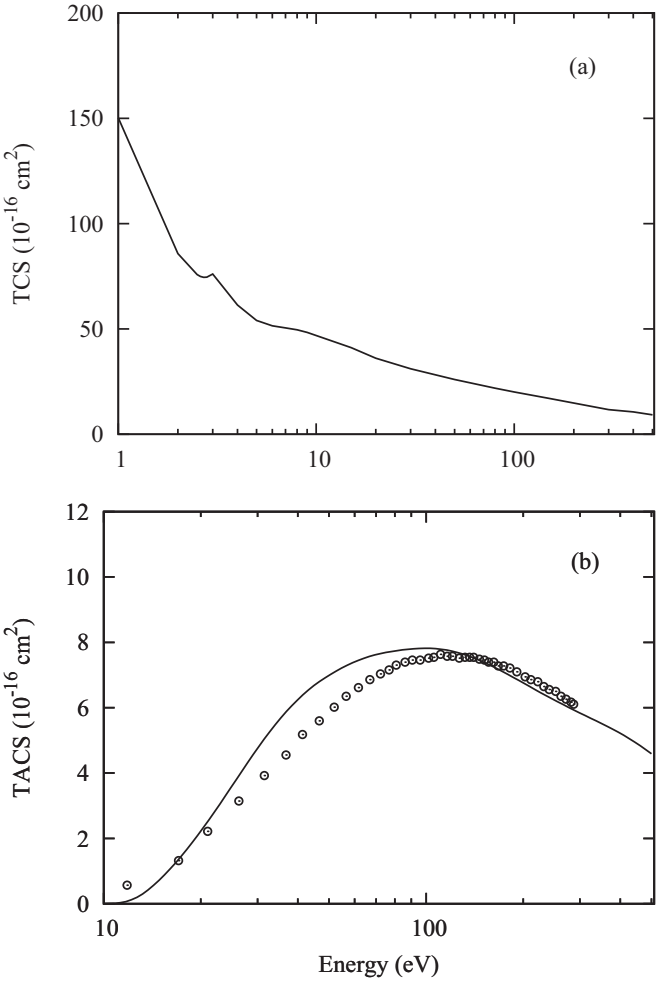

FIG. 5. The (a) TCS and (b) TACS for e^--methyl formate scattering: solid curve, present data calculated using the MCOP; open circles, experimental TICS of Hudson *et al.* [6].

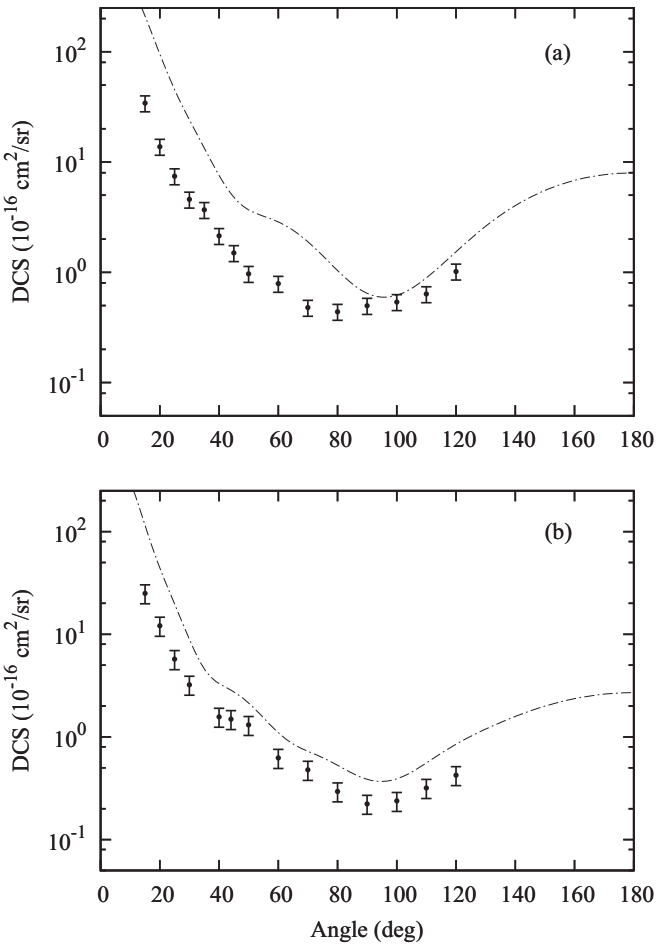

FIG. 6. The DCS for elastic e^--ethyl acetate scattering at (a) 30 eV and (b) 50 eV: dash-dotted curve, present IAM results; closed circles, present experimental results.

symmetry. This resonance also occurs in electron scattering by hydrocarbons [19,20] and is of a $k\sigma^*$ nature, as already discussed by Kimura *et al.* [37]. In contrast, Freitas *et al.* found two structures in the $^2A'$ scattering channel, including one located at around 8 eV. However, both structures were considered spurious and therefore disregarded by them.

In Fig. 5(a) we present our theoretical TCS for electron scattering by methyl formate in the 1–500 eV range. Unfortunately, there are neither theoretical nor experimental results of TCS reported for this target to compare with our data. In Fig. 5(b) the present TACS are compared with experimental TICS of Hudson *et al.* [6] at incident energies from near threshold to 285 eV. In general, there is very good qualitative agreement between our calculated TACS and experimental TICS. Quantitatively, there is also very good agreement for energies above 100 eV. At lower energies, our TACS lie in general above the TICS. This is due to the fact that TACS account for both excitation and ionization channels, while the measured TICS do not include excitation processes. Near threshold, the experimental TICS are larger than our TACS, which may be due to the instability of the trap current regulation below 15 eV, as stated in [6]. For completeness, our MCOP DCS in the 1–20 eV range are shown in Supplemental Material [38].

B. Ethyl acetate

For this molecule, the MCOP calculations would be too involved and therefore comparisons are made only with our theoretical results calculated using the IAM. They are shown in Figs. 6–8. In general, our calculated IAM DCS agree qualitatively well with the present measured results. As expected, the IAM calculations clearly overestimate the experimental DCS at 100 eV and below. This is probably due to the fact that in IAM calculations, the e^--molecule interaction is represented simply by a sum of atomic potentials. Certainly, such an approximation would fail at low incident energies, where the projectile electron has less penetration power into the molecule and so the scattering would be dominated by long-range potentials. Moreover, the IAM calculation, in its usual form, does not include intramolecular multiple-scattering effects (IMSE). The relevance of such effects was investigated by Iga *et al.* [39] for electron scattering by N_2 in the 50–1000 eV range. Those authors showed that even at 300 eV, the IMSE reduce significantly the DCS at small scattering angles. In addition, it is also expected that the

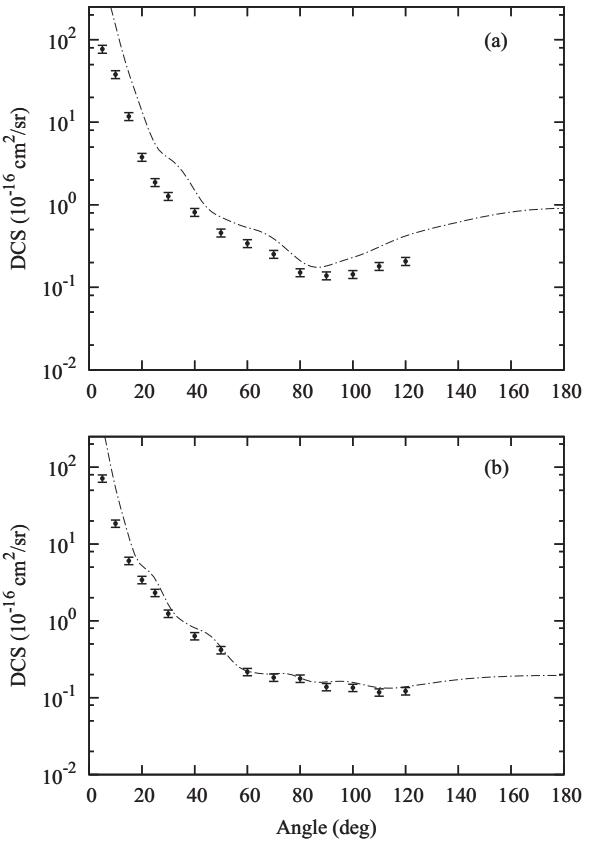

FIG. 7. Same as in Fig. 6 but at (a) 100 eV and (b) 200 eV.

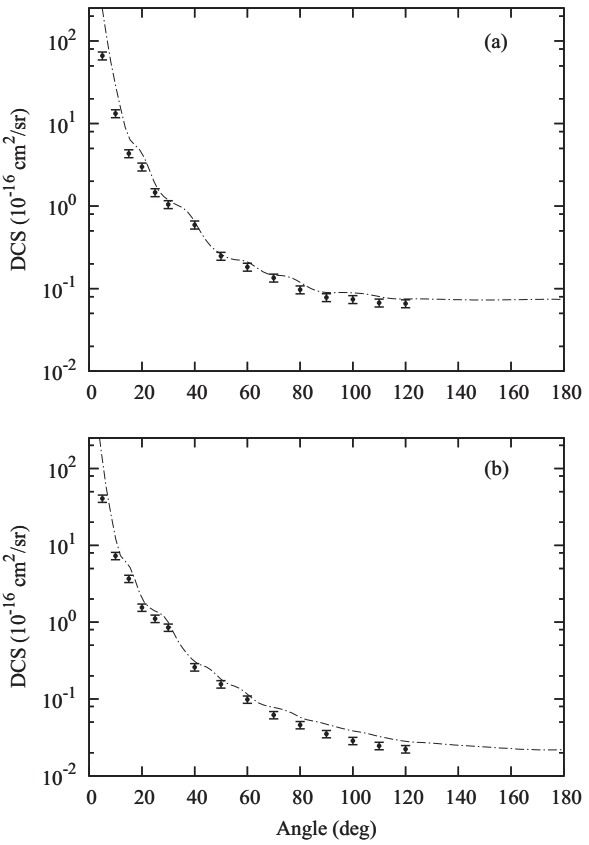

FIG. 8. Same as in Fig. 6 but at (a) 300 eV and (b) 500 eV.

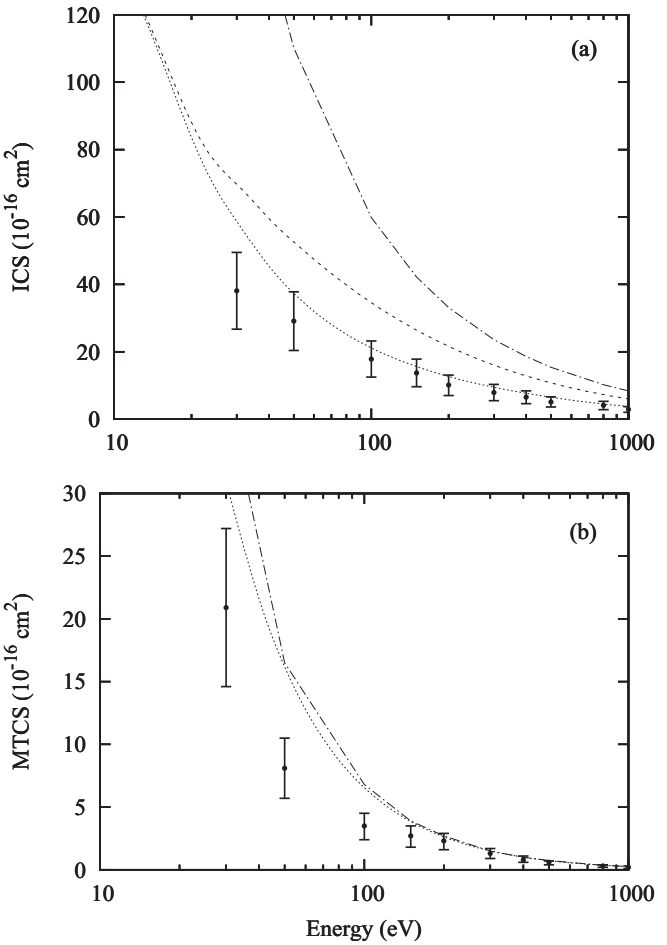

FIG. 9. The (a) ICS and (b) MTCS for elastic e^--ethyl acetate scattering: dash-dotted curve, present calculated data using the IAM; dotted curve, present calculated data using the AR; dashed curve, present TCS data calculated using the AR; closed circles, present experimental data.

IMSE would be more relevant with increasing molecular size (number and weight of atoms). Although the inclusion of IMSE in calculations would significantly improve the agreement between the IAM DCS and experimental results at small scattering angles, their implementation for large molecules is still too involved. Therefore, the IAM DCS would only agree well with experimental data at incident energies where the failure of the above approximations is minimized, which varies from target to target. For this system, even at energies as high as 500 eV, the IAM still strongly overestimates the experimental DCS at small scattering angles.

In Fig. 9 we compare our experimental ICS and MTCS measured in the 30–1000 eV range with those calculated using the IAM. The present theoretical results obtained using the additivity rule (AR) [40] are also shown. Our IAM calculations strongly overestimate the experimental ICS. This fact is directly related to the small-angle behavior of the IAM DCS as stated above. On the other hand, the present AR ICS are in reasonably good agreement with our measured data.

Recently, Blanco and García [41] investigated theoretically the relevance of the interference terms in the IAM. In that

TABLE II. Experimental DCS (in 10^{-16} cm^2/sr), ICS (in 10^{-16} cm^2), and MTCS (in 10^{-16} cm^2) for elastic e^--ethyl acetate scattering. Extrapolated values are given in parentheses.

Angle					E (eV)					
(deg)	30	50	100	150	200	300	400	500	800	1000
					DCS					
3	(123)	(180)	(175)	(110)	(90)	(85)	(80)	(75)	(67)	(47)
5	(111)	(160)	(150)	(90)	71.41	66.22	60.65	40.60	(45)	24.39
10	(70)	(77)	37.87	46.79	18.50	13.24	10.34	7.30	6.43	5.03
15	34.17	25.03	11.74	12.46	6.06	4.33	4.37	3.68	2.02	1.89
20	13.73	12.10	3.77	4.57	3.42	2.99	2.29	1.55	1.36	1.39
25	7.43	5.72	1.87	2.49	2.32	1.46	1.27	1.11	0.788	0.590
30	4.58	3.22	1.27	1.49	1.24	1.05	1.02	0.851	0.381	0.316
40	2.14	1.57	0.812	0.604	0.634	0.593	0.379	0.260	0.177	0.132
50	0.968	1.31	0.457	0.379	0.418	0.248	0.199	0.156	0.084	0.062
60	0.789	0.624	0.340	0.233	0.217	0.183	0.130	0.099	0.047	0.036
70	0.478	0.478	0.252	0.145	0.183	0.135	0.085	0.062	0.032	0.022
80	0.439	0.294	0.151	0.151	0.178	0.097	0.064	0.046	0.022	0.015
90	0.497	0.223	0.138	0.145	0.139	0.078	0.055	0.035	0.014	0.011
100	0.538	0.237	0.144	0.134	0.135	0.074	0.048	0.029	0.012	0.008
110	0.635	0.318	0.179	0.160	0.117	0.067	0.040	0.025	0.010	0.007
120	1.02	0.424	0.207	0.167	0.122	0.066	0.039	0.022	0.008	0.006
130	(1.72)	(0.67)	(0.25)	(0.18)	(0.14)	(0.07)	(0.04)	(0.02)	(0.008)	(0.006)
140	(2.65)	(0.89)	(0.30)	(0.19)	(0.16)	(0.07)	(0.03)	(0.02)	(0.007)	(0.005)
150	(3.64)	(1.12)	(0.35)	(0.21)	(0.17)	(0.07)	(0.03)	(0.02)	(0.007)	(0.005)
160	(4.50)	(1.33)	(0.39)	(0.23)	(0.17)	(0.07)	(0.03)	(0.02)	(0.006)	(0.004)
170	(5.05)	(1.47)	(0.43)	(0.24)	(0.18)	(0.07)	(0.03)	(0.02)	(0.006)	(0.004)
180	(5.25)	(1.52)	(0.44)	(0.25)	(0.18)	(0.07)	(0.03)	(0.02)	(0.006)	(0.004)
					ICS					
	37.9	31.1	17.7	15.3	10.3	8.1	6.9	5.2	4.3	2.9
					MTCS					
	20.7	8.5	3.4	2.6	2.2	1.3	0.84	0.58	0.29	0.22

work they calculated DCS and ICS for both electron and positron scattering by two small targets, namely, H_2 and CH_4, in the 30–300 eV range. Their study suggested that the use of IAM rather than the AR is recommended since the interference effects are not negligible at the intermediate and high energies. Nevertheless, for a number of molecules, the comparison between the experimental ICS with those obtained using the IAM has systematically shown poorer agreement than those of the AR [9,42]. However, this better agreement between experimental and AR ICS may be fortuitous due to the absence of both IMSE and interference terms, which leads to contributions opposite each other. On the other hand, the IAM MTCS agree fairly well with both the AR and experimental MTCS, probably because the contributions of the small-angle DCS to the MTCS are less important.

For completeness, the experimental DCS, ICS, and MTCS in the 30–1000 eV range are listed in Table II. For this system, extrapolated DCS in the angular range not covered in the experiment were also included. At small angles, they were obtained visually and at large angles they followed the trend of the IAM calculations.

V. CONCLUSION

This study reports an experimental investigation on elastic electron collisions with two small esters, methyl formate and ethyl acetate, in a wide energy range. More precisely, absolute DCS, ICS, and MTCS for these targets were measured in the 30–1000 eV range. The present study is mainly motivated by the lack of experimental cross sections for these targets in the literature. In particular, for methyl formate, a theoretical investigation based on the MCOP interaction combined with the Padé approximation was also carried out. Our measured data for methyl formate are in generally good agreement with our theoretical data calculated using the MCOP model. We have also identified a sharp resonance in the $^2A''$ scattering channel at about 3.0 eV. This π^*-type resonance is well known in electron scattering experiments with targets containing a carbonyl group [14,21,36]. In addition, a σ^*-type resonance centered at about 8.0 eV is identified in the $^2A''$ scattering channel.

For ethyl acetate, the comparison of our experimental results is made only with those calculated using the IAM and the AR. Despite very good qualitative agreement, the IAM calculations overestimate the experimental DCS at energies of 100 eV and below.

ACKNOWLEDGMENTS

This research was partially supported by the agencies FAPESP (Brazil), CNPq (Brazil), and CAPES (Brazil). The authors would also like to thank the undergraduate students G. H. Davanzo and G. E. O. Camargo for their valuable help.

[1] G. W. Huber, S. Iborra, and A. Corma, Chem. Rev. **106**, 4044 (2006).

[2] A. Remijam, Y.-S. Shiao, D. N. Friedel, D. S. Meier, and L. E. Snyder, Astrophys. J. **617**, 384 (2004).

[3] S. Liu, D. M. Mehringer, and L. E. Snyder, Astrophys. J. **552**, 654 (2001).

[4] S. Cradock and D. H. Rankim, J. Mol. Struct. **69**, 145 (1980).

[5] I. Ishii and A. P. Hitchcock, J. Electon Spectrosc. Relat. Phenom. **46**, 55 (1988).

[6] J. E. Hudson, Z. F. Weng, C. Vallance, and P. W. Harland, Int. J. Mass Spectrom. **248**, 42 (2006).

[7] I. Iga, M. T. Lee, M. G. P. Homem, L. E. Machado, and L. M. Brescansin, Phys. Rev. A **61**, 022708 (2000).

[8] P. Rawat, I. Iga, M. T. Lee, L. M. Brescansin, M. G. P. Homem, and L. E. Machado, Phys. Rev. A **68**, 052711 (2003).

[9] M. G. P. Homem, R. T. Sugohara, I. P. Sanches, M. T. Lee, and I. Iga, Phys. Rev. A **80**, 032705 (2009).

[10] M. G. P. Homem, I. Iga, R. T. Sugohara, I. P. Sanches, and M. T. Lee, Rev. Sci. Instrum. **82**, 013109 (2011).

[11] R. T. Sugohara, M. G. P. Homem, I. P. Sanches, A. F. de Moura, M. T. Lee, and I. Iga, Phys. Rev. A **83**, 032708 (2011).

[12] M.-T. Lee, G. L. C. de Souza, L. E. Machado, L. M. Brescansin, A. S. dos Santos, R. R. Lucchese, R. T. Sugohara, M. G. P. Homem, I. P. Sanches, and I. Iga, J. Chem. Phys. **136**, 114311 (2012).

[13] R. T. Sugohara, M. G. P. Homem, I. Iga, G. L. C. de Souza, L. E. Machado, J. R. Ferraz, A. S. dos Santos, L. M. Brescansin, R. R. Lucchese, and M.-T. Lee, Phys. Rev. A **88**, 022709 (2013).

[14] M. G. P. Homem, I. Iga, L. A. da Silva, J. R. Ferraz, L. E. Machado, G. L. C. de Souza, V. A. S. da Mata, L. M. Brescansin, R. R. Lucchese, and M.-T. Lee, Phys. Rev. A **92**, 032711 (2015).

[15] S. K. Srivastava, A. Chutjian, and S. Trajmar, J. Chem. Phys. **63**, 2659 (1975).

[16] T. W. Shyn and G. R. Carignan, Phys. Rev. A **22**, 923 (1980).

[17] R. H. J. Jansen, F. J. de Heer, H. J. Luyken, B. van Wingerden, and H. J. Blaauw, J. Phys. B **9**, 185 (1976).

[18] R. D. DuBois and M. E. Rudd, J. Phys. B **9**, 2657 (1976).

[19] P. Rawat, M. G. P. Homem, R. T. Sugohara, I. P. Sanches, I. Iga, G. L. C. de Souza, A. S. dos Santos, R. R. Lucchese, L. E. Machado, L. M. Brescansin, and M.-T. Lee, J. Phys. B **43**, 225202 (2010).

[20] G. L. C. de Souza, M.-T. Lee, I. P. Sanches, P. Rawat, I. Iga, A. S. dos Santos, L. E. Machado, R. T. Sugohara, L. M. Brescansin, M. G. P. Homem, and R. R. Lucchese, Phys. Rev. A **82**, 012709 (2010).

[21] J. R. Ferraz, A. S. dos Santos, G. L. C. de Souza, A. I. Zanelato, T. R. M. Alves, M.-T. Lee, L. M. Brescansin, R. R. Lucchese, and L. E. Machado, Phys. Rev. A **87**, 032717 (2013).

[22] F. A. Gianturco, R. R. Lucchese, and N. Sanna, J. Chem. Phys. **102**, 5743 (1995).

[23] A. R. Edmonds, *Angular Momentum and Quantum Mechanics* (Princeton University Press, Princeton, 1960).

[24] N. T. Padial and D. W. Norcross, Phys. Rev. A **29**, 1742 (1984).

[25] M.-T. Lee, I. Iga, L. E. Machado, L. M. Brescansin, E. A. y Castro, I. P. Sanches, and G. L. C. de Souza, J. Electron Spectrosc. Relat. Phenom. **155**, 14 (2007).

[26] E. A. y Castro, G. L. C. de Souza, I. Iga, L. E. Machado, L. M. Brescansin, and M.-T. Lee, J. Electron Spectrosc. Relat. Phenom. **159**, 30 (2007).

[27] G. Staszewska, D. W. Schwenke, and D. G. Truhlar, Phys. Rev. A **29**, 3078 (1984).

[28] S. Hara, J. Phys. Soc. Jpn. **22**, 710 (1967).

[29] M. W. Schmidt, K. K. Baldridge, J. A. Boatz, S. T. Elbert, M. S. Gordon, J. H. Jensen, S. Koseki, N. Matsunaga, K. A. Nguyen, S. Su, T. L. Windus, M. Dupuis, and J. A. Montgomery, J. Comput. Chem. **14**, 1347 (1993).

[30] http://cccbdb.nist.gov.

[31] P. G. Burke, N. Chandra, and F. A. Gianturco, J. Phys. B **5**, 2212 (1972).

[32] L. M. Brescansin, L. E. Machado, M.-T. Lee, H. Cho, and Y. S. Park, J. Phys. B **41**, 185201 (2008).

[33] L. E. Machado, L. M. Brescansin, I. Iga, and M.-T. Lee, Eur. Phys. **33**, 193 (2005).

[34] M.-T. Lee and L. C. G. Freitas, J. Phys. B **13**, 233 (1983).

[35] T. C. Freitas, M. T. do N. Varella, R. F. da Costa, M. A. P. Lima, and M. H. F. Bettega, Phys. Rev. A **79**, 022706 (2009).

[36] M. G. P. Homem, I. Iga, G. L. C. de Souza, A. I. Zanelato, L. E. Machado, J. R. Ferraz, A. S. dos Santos, L. M. Brescansin, R. R. Lucchese, and M.-T. Lee, Phys. Rev. A **90**, 062704 (2014).

[37] M. Kimura, O. Sueoka, A. Hamada, and Y. Itikawa, Adv. Chem. Phys. **111**, 537 (2007).

[38] See Supplemental Material at http://link.aps.org/supplemental/10.1103/PhysRevA.93.032711 for the MCOP DCS in the 1–20 eV range.

[39] I. Iga, R. A. Bonham, and M.-T. Lee, J. Mol. Struct. **468**, 241 (1999).

[40] D. Shi, J. Sun, Y. Liu, and Z. Zhu, J. Phys. B **41**, 025205 (2008).

[41] F. Blanco and G. García, Chem. Phys. Lett. **635**, 321 (2015).

[42] I. P. Sanches, R. T. Sugohara, L. Rosani, M.-T. Lee, and I. Iga, J. Phys. B **41**, 185202 (2008).